Geotechnical Aspects of Underground Construction in Soft Ground – Viggiani (ed)
© 2012 Taylor & Francis Group, London, ISBN 978-0-415-68367-8

Understanding ground deformation mechanisms during multi-propped excavation in soft clay

S.Y. Lam, S.K. Haigh & M.D. Bolton
University of Cambridge, UK

ABSTRACT: To maximize the utility of high land cost in urban development, underground space is commonly exploited, both to reduce the load acting on the ground and to increase the space available. The execution of underground constructions requires the use of appropriate retaining wall and bracing systems. Inadequate support systems have always been a major concern, as any excessive ground movement induced during excavation could cause damage to neighboring structures, resulting in delays, disputes and cost overruns. Experimental findings on the effect of wall stiffness, depth of the stiff stratum away from the wall toe and wall toe fixity condition are presented and discussed.

1 INTRODUCTION

To better understanding on the effects of excavation on the movement of the surrounding ground, the direct method is to carry out physical tests and observe them. Centrifuge model tests of deep excavations in slightly over-consolidated soft clay have been carried out using a newly developed testing system, in which the construction sequence of a multi-propped wall for deep excavation can be properly simulated in flight.

2 CENTRIFUGE TESTING

2.1 *Experimental testing programme and setup*

Figure 1 shows the experimental setup of the present study. The rectangular model container is made of aluminum alloy with internal dimensions 790 mm in length, 180 mm in width and 470 mm in depth. The front face of the container consists of a Perspex window, which enables the whole testing process to be monitored by cameras mounted in front. As an increase in soil self-weight leads to an increase in excess pore pressure, the model ground first had to undergo about 5 hours of reconsolidation until at least 90% of the consequential consolidation was achieved. The degree of consolidation was monitored by judging whether pore pressure transducer (PPT) readings were approaching their hydrostatic state. The excavation was then started. The in-flight excavator operated at a rate of 10 mm/s horizontally and with 4 mm vertical increments (Lam et al., 2010). In order to achieve realistic quasi-undrained responses, the excavation process should be finished within a reasonably short period of time. Figure 4 shows the progress of excavation in all tests. Excavation to an excavation depth of 5.5 m finished within 30–40 minutes (72–96 days at prototype scale), which is similar to the typical rate of excavation in the field. Table 1 summarizes the objectives and test descriptions of the test programme.

2.2 *Prop installation and gate system*

Instrumentation comprising of pore pressure transducers in the soil, earth pressure cells on the retaining wall, bending moment strain gauges on the wall, load cells on the props and linear variable transformers for displacement measurements were installed. Digital cameras were mounted in front of the Perspex window for particle image Velocimetry (PIV) purposes (White and Take, 2002) and LED arrays were situated to illuminate the clay cross-section without causing glare, or shadows. In this paper, only pore pressure and PIV data was discussed.

The vertical plane through the center of an excavation could be regarded as a plane of symmetry. A "gate wall" (as shown in Figure 1) aimed to represent this plane of symmetry, so that only one side of the excavation needed to be modeled. A prop installation sub-system was designed to provide in-flight support, initially to the gate wall and ultimately to the retaining wall, during the experiment. Three pairs of cylinders were mounted on a rigid support frame and positioned at 0 mm, 36 mm and 72 mm below the initial clay surface. Props were driven via pistons in the cylinders which were actuated through a hydraulic/pneumatic control system.

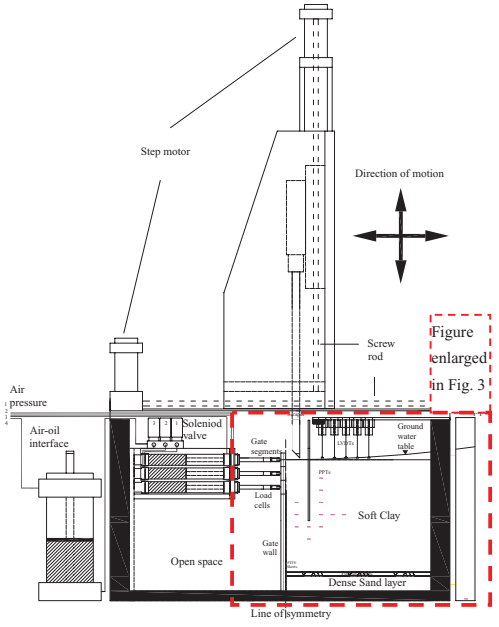

Figure 1. Schematic diagram of experimental setup with in-flight excavator.

Backward pressure inlets were connected to a compressed air source for retreating the cylinders. Forward pressure inlets were connected to an oil pressure reservoir so that they could provide a similar propping force at each excavation level. Each level of props was controlled individually through solenoid valves. The oil supply manifold was connected to an air-oil interface through a needle valve which was used to control the rate of advance of each pair of props, in sequence. Compressed air acting on the front face of the pistons was transmitted from an external compressor and regulator, and was supplied to the centrifuge through a pneumatic coupling. Before the experiment, the system was saturated with hydraulic oil. The prop stiffness was obtained by conducting axial-load displacement tests in a loading rig. The target stiffness of a fully-saturated prop was found to be about 1.66 kN/mm.

Figure 2 shows the gate system. At the start of the experiment, three pairs of sacrificial gates, each 36 mm high, sat on the top of the gate wall. They acted as a support to retain the soil to be excavated. The gates were temporarily supported by the pairs of cylinders throughout the initial reconsolidation stage before excavation. The forces required to support the gate segments were monitored by axial load cells attached at the end of each prop. Figure 2 shows the sequence of the first excavation stage. At the start of excavation, the first pair of cylinders was retracted so that the first layer of gates was in an unstable condition and was easily knocked down by the scraper of the in-flight excavator. The in-flight excavator then makes a 4 mm cut into the soil, which was scraped off into the open space inside the cylinder support system. The scraper then returned to its initial position and made another 4 mm cut, repeating until the excavation level reached the top of the second level of gates. At that moment, the first level of props was pressurized again to support the retaining wall. The prop force required could be adjusted by looking at the readings given by the prop load cells. This completed the first stage of excavation. As the scraper was specially made in an inverted T-shape, it could continue scraping below the first pair of props. The second and third stages of excavation could therefore proceed by repeating the same steps carried out for the first level.

2.3 *Preparation of model ground*

A base layer of fine Fraction E sand was formed by pluviation using an automatic pouring machine (Madabhushi *et al*., 2006). A constant fall-height of 600 mm was used to achieve a uniform layer with a relative density above 95% and a dry unit weight of 16.0 kN/m^3. Saturation of the sand was effected by connecting the bottom drainage hole to a standpipe filled with water. Since one of the objectives of these particular tests was to monitor excavation in soft clay and to compare different bracing schemes, lightly over-consolidated kaolin clay was used in the models. Clay powder was mixed with water to about twice the liquid limit (i.e. 120% moisture content), the mixing taking place under vacuum for at least two hours. The clay slurry was carefully poured on the bearing layer.

Table 1. A summary of centrifuge testing programme.

Test		Objective	D (mm)	Prop stiffness (kN/mm)	System stiffness $EI_{wall}/\gamma_w s^4$	Toe fixity
1	Floating rigid wall with stiff props	Baseline	300	1.66	2860	Free
2	Floating flexible wall with stiff props	Wall stiffness	300	1.66	106	Free
3	Fixed-base flexible wall with base slab	Fixed wall toe	300	1.66	106	Fixed
4	Fixed-base flexible wall in shallow clay	Clay thickness	160	1.66	106	Free

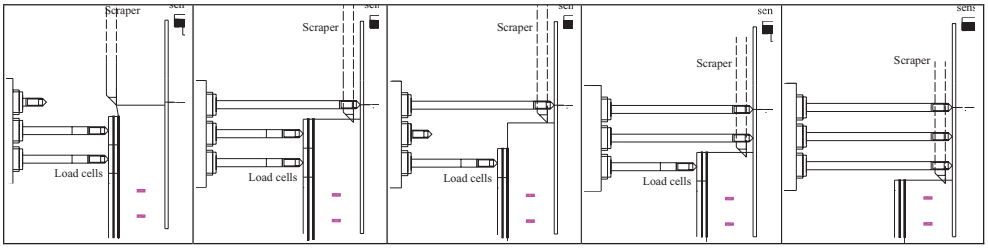

Figure 2. Modeling sequences of excavation.

The container was placed in a hydraulic press, and pressure was applied to the clay in six loading steps (to 2 kPa, 5 kPa, 10 kPa, 20 kPa, 40 kPa and 80 kPa, and 160 kPa).The final pressure of 160 kPa was intended to achieve an estimated c_u of 25 kPa for the clay at mid-depth in the centrifuge model when it had swollen back into equilibrium at 60 g.

When the settlement of the clay in the press became steady under 80 kPa, the clay was unloaded. Nine PPTs were inserted through pre-drilled openings in the back wall of the container. PPTs were installed through 90 mm long holes augured horizontally into the clay using a hand drill. The final locations of the PPTs are shown in Figure 3. After installation, loading was brought back to 80 kPa. After equilibration, the consolidation pressure was further increased to 160 kPa. After settlement was steady, the pressure was reduced again to 80 kPa and the clay was allowed to swell into equilibrium. Removal of this final pressure was known to be possible without drawing air into the clay.

The loading plate was removed. After trimming the clay surface, the resulting clay thickness was 295 mm. The front wall of the model container was then removed. The clay and base layer were then removed from that half of the package that would contain the cylinder support system. The retaining wall, in the particular test to be described here, is made of either a 2 mm or a 6 mm thick aluminum alloy plate with an equivalent stiffness (EI) of 10.4 MNm/m^2 or 280.8 MNm/m^2 at prototype scale, respectively. These walls simulate a sheet pile wall (US steel, PDA-27) and a 0.9 m thick diaphragm wall in the field. Greased wiper seals were used to prevent water from seeping past the sides of the wall and to ensure a free sliding condition with minimal friction. The wall was installed at a depth of 160 mm (equivalent to 10.6 m prototype). A set of vertical guides and a cutter were used to dig a trench with the same thickness as the wall. The wall was then pushed into the trench using a vertical guide. With the clay cross-section uppermost, grains of black-dyed fraction E sand were blown onto the clay to provide PIV texture. Lubricant was then applied to the Perspex window to reduce

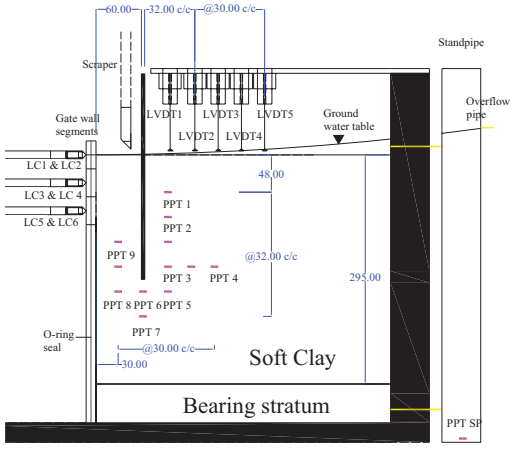

Figure 3. Positions of instruments on model package.

friction against the soil cross-section. The Perspex window was then bolted to the main body of the container. LVDTs were assembled at 30 mm spacing intervals from the wall to measure the soil settlement profile. Finally, the water table in the clay was to be maintained at the ground surface by permitting overflow from a stand pipe which would be supplied continuously throughout the experiment. Two 8 megapixels cameras took pictures throughout the experiment with the provision of suitable lighting. The detailed locations of the instrumentation are shown in Figure 3.

2.4 *Excavation test procedure*

The in-flight excavator was bolted above the model container, and the integrated assembly was transferred onto the centrifuge swing platform. This was fixed to the torsion-bar catches which permit the package to rotate into a fixed-end condition at a centrifuge acceleration of about 10 g. The model was then brought to its scale acceleration of 60 g. There are three test phases for a typical centrifuge test of deep excavation–reconsolidation, in-flight

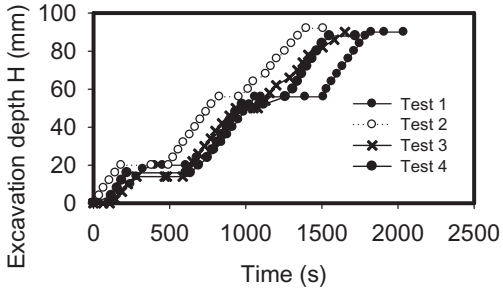

Figure 4. Progress of excavations.

excavation, and long-term equilibration. In this paper, only results on the excavation phase are presented.

As an increase in soil self-weight leads to an increase in excess pore pressure, the model ground first had to undergo about 5 hours of reconsolidation until at least 90% of the consequential consolidation was achieved. The degree of consolidation was monitored by judging whether pore pressure transducer (PPT) readings were approaching their hydrostatic state.

The excavation was then started. The in-flight excavator operated at a rate of 10 mm/s horizontally and with 4 mm vertical increments. In order to ensure that realistic quasi-undrained responses were observed, the excavation process should be finished within a reasonably short period of time. Figure 4 shows the progress of excavation in all tests. Excavation to an excavation depth of 5.5 m finished within 30–40 minutes (72–96 days at prototype scale), which is similar to the rate of excavation in the field.

Following excavation, the test was allowed to continue and excess pore pressures that had been generated by excavation were observed to dissipate as long term deformations were monitored.

3 RESULTS AND DISCUSSIONS

3.1 *Pore pressure behavior during excavation*

As the excavation proceeds, the ground water level in front of the wall was lowered simultaneously. The bottom drainage layer was connected to a standpipe which maintains a hydrostatic water pressure measured from soil surface at the back of the wall throughout each test. Water flow through the sides of the wall was prevented by greased seals. Under such condition, downward seepage at the backside of the wall and upward seepage in front of the wall in long terms should be expected.

Figure 5(a) shows the variation of pore water pressure during excavation using a 0.9 m thick diaphragm wall in Test 1. In front of the wall, there was a negative pore pressure built-up (PPT 9 and PPT 8) due to the reduction in total mean stresses during excavation. The magnitude of the negative pore pressures was smaller than the effective over-burden pressure lost in excavation. This is owing to the fact that the negative pore pressure were cancelled out by the positive pore pressures generated by shear deformation of clay. On the other hand, the change in pore pressure measured at the back of the retaining wall (PPT 1, PPT 2 and PPT 3) was relatively small because the stiff prop supports limited lateral wall deformation and thus limited reduction in lateral horizontal stress.

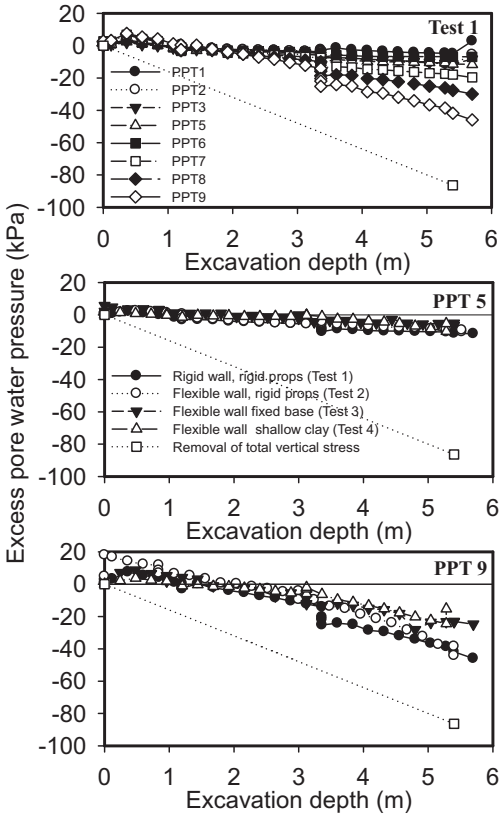

Figure 5. Variation of water pressure (a) for Test 1 (PPT 1–9) (b) at bottom of excavation site (PPT9) for tests (c) at mid-depth of wall on retained side (PPT5) for all tests.

Comparison of variation of pore water pressure underneath the excavation (PPT 9) for different centrifuge tests is made in Figure 5(b). The removal of over-burden stress is plotted on the same graph for comparison. As described earlier, the negative pore pressure by removal of the over-burden stress is cancelled out by the generation of positive excess pore pressure by shear deformation of clay. The decrease

in rate of pore pressure reduction for Test 2, 3 and 4 is ascribed to more extensive excavation induced shear strain induced by flexible wall bulging and thus generation of positive excess pore water pressure. On the other hand, a similar comparison carried out for pore water pressure below the wall toe on the retained side (PPT5) (Figure 5(c)) shows very similar rate of development of excess pore pressure for all cases. The influence of vertical over-burden stress removal is cancelled out by the shear induced positive excessive fluid pressure in a similar order of magnitude for all tests.

3.2 *Ground settlement and wall deflection*

The characteristics of wall deflection and ground settlement profile during undrained excavation is a vital parameter for assessing potential damages to neighbouring structures and buried services. In an ideal excavation process, the support level is installed at an early stage in order to minimize cantilever movement of the wall. However, this may not be always possible in practice due to a variety of site constraints and construction sequences. In the present studies, the excavation procedures initiated with a cantilever stage of excavation, which was then followed by singly propped and finally multi-propped excavation. Ground movements were captured by the PIV technique. Results of ground settlement profile at some discrete measurement point away from the retaining wall monitored by LVDTs are also included for comparisons for Test 2. In general, the results obtained by LVDTs and the PIV technique are comparable, which ensures that the model is testing under plane strain condition properly.

Figure 6 shows the development of lateral wall displacement and ground settlement of a deep excavation using flexible wall (Test 2). Consistent with results shown by previous researchers (Powrie, 1986), rotation of wall about the wall toe was observed in the cantilever excavation stage. Maximum incremental cantilever wall deflection of about 10 mm was observed at the wall crest in prototype scale (0.167 mm in model scale), which is equivalent to 0.2% of average engineering shear strain in the 45 degree triangular zone behind the wall according to Osman and Bolton (2004).

Considering the incremental deformations of a multi-propped wall supporting a deep excavation in soft, undrained clay, at each stage of excavation the incremental displacement profile of the ground and the wall below the lowest prop was assumed to be a cosine function by O'Rourke(1993) as

$$\delta w = \frac{\delta w_{\max}}{2}\left(1-\cos\left(\frac{2\pi y}{\lambda}\right)\right) \quad (1)$$

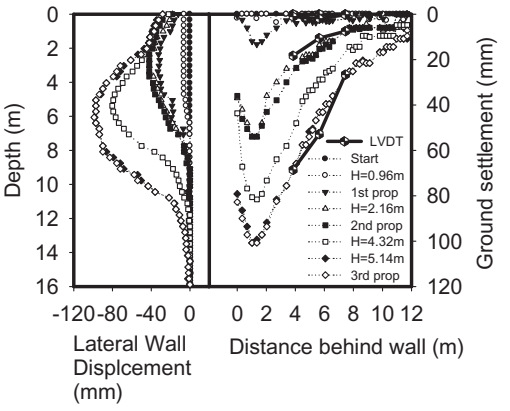

Figure 6. Development of wall deformation and ground settlement with progress of excavation (Test 2).

where δw is the incremental wall displacement at any distance y below the lowest support, δw_{max} is its maximum value, and λ is the wavelength of the deformation, regarded as proportional to the length s of the wall below the lowest level of current support $\lambda = \alpha s$.

O'Rourke (1993) defined the wavelength of the deformation as the distance from the lowest support level to the fixed base of the wall. Osman and Bolton (2006) suggested a definition for the wavelength of the deformation based on wall end fixity. For walls embedded into a stiff layer beneath the soft clay, such that the wall tip is fully fixed in position and direction, the wavelength was set equal to the wall length ($\alpha = 1$). For short walls embedded in deep soft clay, the maximum wall displacement occurs at the tip of the wall so the wavelength was taken as twice the projecting wall length ($\alpha = 2$). Intermediate cases were described as restrained-end walls ($1 < \alpha < 2$). For the excavation in deep soft clay layer, the α value is found to be 1.3–1.5. It should be noted that this value would be a function of soil-wall relative stiffness.

The settlement tough occurs at some distance away from the wall, which is slightly different from the triangular tough pattern observed by Powrie (1986). The subsequent stages of excavation involve deep-seated soil flow mechanism and bulging of the retaining wall below the lowest level of struts. The maximum incremental lateral wall displacement for the second and the third stages were 30 mm and 90 mm (0.5 mm and 1.5 mm in model scale), respectively. These movements were equivalent to about 0.6% and 1.5% of average incremental engineering shear strain, respectively, within the deformation zone according to Bolton et al. (2008).

These findings once again showed the importance of small strain stiffness of over-consolidated soil on analyzing multi-propped excavation problem. The development of settlement toughs is complicated by the superposition of deep settlement tough near the wall. This observation is consistent with the general observation given by Clough and O'Rourke (1990) that the settlement tough of a multi-propped excavation is bounded by a trapezoidal zone extended up to 2 times the maximum excavation depth. It is also noted that the areas underneath the two curves are roughly equal, consistent with zero volumetric strain in undrained conditions.

3.3 *Effect of wall stiffness*

Clough et al. (1989) proposed a semi-empirical procedure for estimating movement at excavations in clay in which the maximum lateral wall movement; δ_{hm} is evaluated relative to factor of safety (FS) and system stiffness, which is defined as follows:

$$\textit{System stiffness } (\eta) = EI/\gamma_w h^4 \tag{3}$$

where EI is the flexure rigidity per unit width of the retaining wall, γ_w the unit weight of water and h the average support spacing.

It should be emphasized that FS is used as an index parameter. The system stiffness is defined as a function of the wall flexural stiffness, average vertical separation of supports, and unit weight of water, which is used as a normalizing parameter.

As a result, it is very interesting to know if the normalized wall deformation would change by varying system stiffness and keeping other parameters unchanged in a centrifuge test. The wall deformation profile is shown in Figure 7.

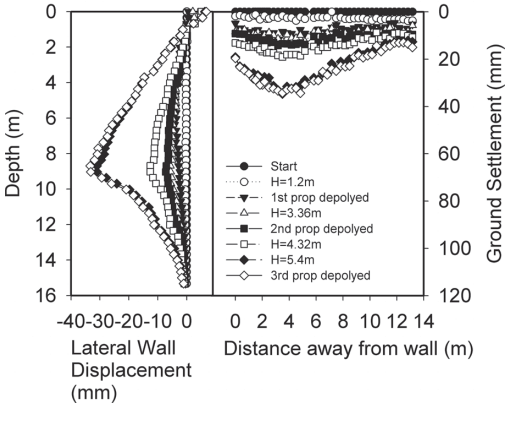

Figure 7. Development of wall deformation and ground settlement with progress of excavation (Test 1).

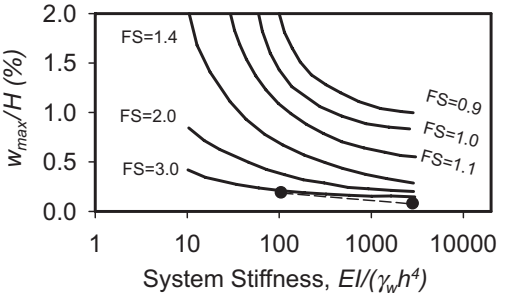

Figure 8. Variation of wall deformation with system stiffness following Clough et al. (1989).

The wall thickness of rigid retaining wall is 3 times that of its flexible counterpart. Since the moment of inertia I term is proportional to cubic of the thickness of wall, the system stiffness differed by a factor of 27. Figure 8 shows δ_{hm} plotted relative to system stiffness for various FS. The factor of safety for the present excavation geometry and soil profile is calculated by the following expression.

$$FS = \frac{(N_c)(c_u)}{H\left(\gamma - \frac{2}{\sqrt{2}}\frac{c_u}{B}\right)} = \frac{(6)(27)}{5.4\left(16 - \frac{2}{\sqrt{2}}\frac{27}{12}\right)} = 2.34 \tag{4}$$

The system stiffness of the rigid wall is calculated to be 2850 whereas that of the flexible wall is 106. The black circles in Figure 8 show the results of the present study. This slight underestimation of wall deformation indicates that system stiffness might be a good measure for quantifying performance of wall deformation for excavation cases. However, the use of factor of safety to quantify wall deformation ignores small strain non-linear stiffness of the soil and also the incremental nature of the construction.

3.4 *Effect of depth to stiff bearing stratum*

Mana and Clough (1981) presented parametric studies on the effect of depth to the bearing stratum on maximum lateral wall displacement for fixed base wall. Results showed that movements increase with excavation width and depth to the bearing stratum. The magnitude of lateral wall displacement increases by a factor of 1.5 when the depth to the stiff layer doubles. However, soils are considered to be elastic which implies that the local development of plastic strain is not possible and over-prediction of soil movements. Jen (1998) investigated into the same issue again with a more sophisticated numerical constitutive model i.e. the MIT-E3 model. Parametric studies

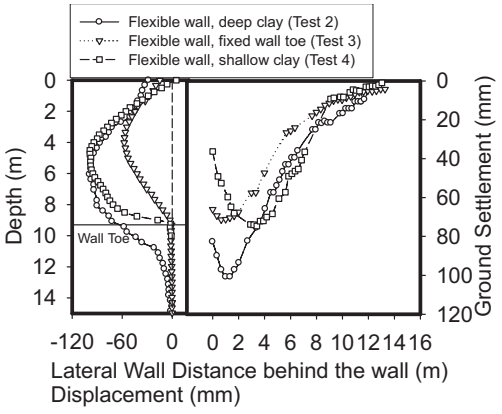

Figure 9. Wall deflection and ground settlement profile for excavation using flexible wall (Test 2, 3 and 4).

on the effect of depth to the hard stratum on lateral wall displacement for excavation using floating wall were carried out. Results show that the depth of end stratum only affects wall deflection below the excavation level, especially the wall toe. On the other hand, shallower clay would have a stronger impact on the distribution of far-field ground settlement. As the location of the rigid base become shallower, the trail of the settlement trough tapers off much more rapidly. The distance for the tapering off is roughly equal to the depth of stiff stratum.

Figure 9 shows the final wall displacement and ground settlement profiles of excavation in shallow clay (Test 4). Since the wall toe is not fixed to the base, wall toe rotation and wall bulging movement are the major deformation mode shape. The lateral wall deformation mode shape is very much similar to that of Test 2 except that the length of the bulge is limited to the depth of stiff layer. The evolution of the soil displacement mechanism is illustrated in Figure 10 for different stages of excavation. The introduction of the first pair of pre-loaded props induces much inward displacement at the wall crest (as shown in Figure 10(a)). The deformation mechanism changed to a free bulging mode which is equivalent to loading a simply supported beam being held vertically. It is the stage that much wall rotation can be developed since there is no moment restraint for props at the wall crest (as shown in Figure 10(b)). After the introduction of the second props, the wall length below the lowest prop is bending moment restrained at the prop location. As an effect, not much wall rotation at the lowest prop location could be observed for excavation stage 3 (Figure 10(c)). The maximum lateral wall displacement for the second and the third stages

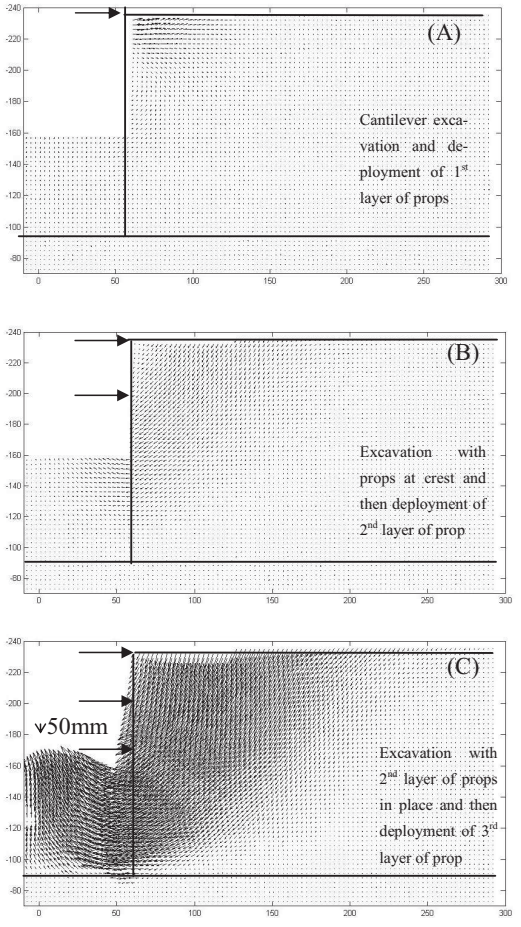

Figure 10. Incremental displacements for different stage of excavation for Test 4.

were 45 mm and 100 mm, respectively. These movements were equivalent to about 0.9% and 2% of average overall engineering shear strain, respectively, within the deformation zone according to Bolton et al. (2008).

Compared with the deformation mechanism of excavation test in deep soft clay, two major observations are spotted. Firstly, the amount of maximum wall displacement is not affected by the depth to the stiff stratum. The difference in the two tests is within 10%. This is comparable to the observation by numerical simulated result by Jen (1998) suggesting that the maximum wall movement would differ only by 20% when the depth of stiff layer increase from 5 m to over 50 m below wall toe. Secondly, the settlement profile of the present test does show a much rapid tapering off as the distance get further away from wall. This observation echoes the results simulated by FEA by Jen (1998).

This implies that an engineer who wants to control the extent of excavation induced movement can consider fixing wall toe with ground improvement methods.

3.5 *Effect of wall toe fixity conditions*

For deep excavation in soft ground, the maximum wall deflection of the retaining wall usually occurs at the final excavation level. To limit wall deflection at this level, ground improvement techniques (e.g. Jet-grouting) are usually employed prior to an excavation. A common approach is to improve the entire soil layer within the excavation zone below the excavation level to fix the wall toe. In the present study, a centrifuge test (Test 3) is carried out to understand how an infinitely stiff fixed base slab layer at the wall toe would affect the deformation mechanism.

Figure 9 shows the effectiveness of a fixed based wall for controlling the lateral wall displacement and ground settlement of excavations. Since the wall toe is fixed to the base, only wall bulging movement is allowed as the deformation mode shape. The lateral wall deformation mode shape is very much similar to that of Test 2 except the fact that a bending moment restraint is being imposed at the wall toe. The maximum lateral wall displacement for the second and the third stages were 40 mm and 65 mm, respectively. These movements were equivalent to about 0.8% and 1.3% of average overall engineering shear strain, respectively, within the deformation zone. In effect, the wall toe fixity restraint controlled lateral soil deformation below final excavation level and the extent of the soil settlement tough away from the wall.

Following Clough et al. (1989) approach, the incremental wall displacement can be generally represented by a normalized wall displacement and depth below lowest prop relationship normalized with wavelength of deformation (Eq.2) shown in Figure 11. Results show that the normalized curves for both floating and fixed base wall broadly follow the cosine curve. The assumed deformation mode shape is proven to be a good representation of a typical wall bulging displacement profile below the lowest prop for multi-prop deep excavation stages.

4 CONCLUDING REMARKS

Maximum lateral wall displacement of a floating support system is a function of the flexural stiffness of the retaining wall. Tripling the thickness of the floating wall reduces maximum wall displacement by 65%, which might not be considered as an economical approach. The depth to the stiff stratum away from the wall toe of a floating flexible wall system does not have a significant effect on maximum wall displacement for floating walls. The wall toe fixity condition is critical in controlling soil deformation below final excavation level and the extent of development of ground surface settlement away from the wall. Should stringent criteria for controlling ground movement during deep basement construction be applied, designers by all means have to restrict wall toe movement either by introducing a base grout or keying the wall toe into a stiff stratum.

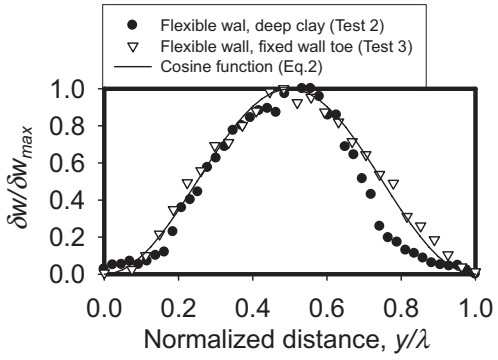

Figure 11. Variation of normalized incremental displacement with distance below the lowest prop.

ACKNOWLEDGEMENTS

The authors would like to acknowledge Mr. John Chandler, Mr. Richard Adams, Mr. Kristian Pether and Mr. Chris McGinnie, the technicians of the Schofield Center, University of Cambridge for their dedication to the project.

REFERENCES

Bolton, M.D., Lam, S.Y. & Osman, A.S. (2008). Supporting excavations in clay-from analysis to decision-making. Special Lecture, *6th International Symposium of Geotechnical Aspects of Underground Construction in Soft Ground.* April, Shanghai.

Clough, G.W. & O'Rourke, T. D., (1990). Construction induced movements of in situ walls. In Proc. Design and performance of earth retaining structure, ASCE Special conference, Ithaca, New York, pp 439–470.

Clough, G.W. & Smith, E.W. and Sweeney, B.P.(1989) Movement control of excavation support system by iterative design. *Foundation Engineering Current Principles and Practices*, Vol.2 ASCE, New York, NY, 1989, pp 869–882.

Jen, L. C. (1998). The design and performance of deep excavation in clay. *Ph.D thesis*, MIT.

Lam, S.Y., Elshafie, M.Z.E.B., Haigh, S.K. & Bolton, M.D. (2010). Development of a new apparatus for modeling deep excavation related problems in geotechnical centrifuge. *ASTM Geotechnical Testing Journal*. (in Press)

Madabhushi, S.P.G., Houghton N.E., & Haigh S.K. (2006). A new automatic sand pourer for model preparation at University of Cambridge. Proc. *ICPMG'2006,* Hong Kong, pp 217–222.

Mana, A.I. & Clough, G.W. (1981). Prediction of movements for braced cuts in clay. ASCE *Soil Mechanics and Foundations Division Journal,* 107(6): 759–777.

Osman, A.S. & Bolton, M.D. (2004). A new design method for retaining walls in clay, *Canadian Geotechnical Journal*, 41(3): 453–469.

Osman, A.S. & Bolton, M.D. (2006). Ground movement predictions for braced excavations in undrained clay. *J. Geotech. & Geoenvir. Engrg.,* ASCE, Vol. 132, No. 4, April 1, 2006.

O'Rourke, T.D. (1993). Base stability and ground movement prediction for excavations in soft clay. *Retaining structures,* Thomas Telford, London, 131–139.

Powrie, W. (1986). The behaviour of diaphragm walls in clay *Phd thesis*, University of Cambridge.

White, D.J. & Take, W.A. (2002). GeoPIV: Particle image velocimetry (PIV) software for use in geotechnical testing, *Technical Report CUED/D-SOILS/TR322*, October 2002, University of Cambridge.